Multiple cell-type interactions drive invariant NKT cell hepatitis

VISUAL ABSTRACT

Multiple cell-type interactions drive invariant NKT cell hepatitis

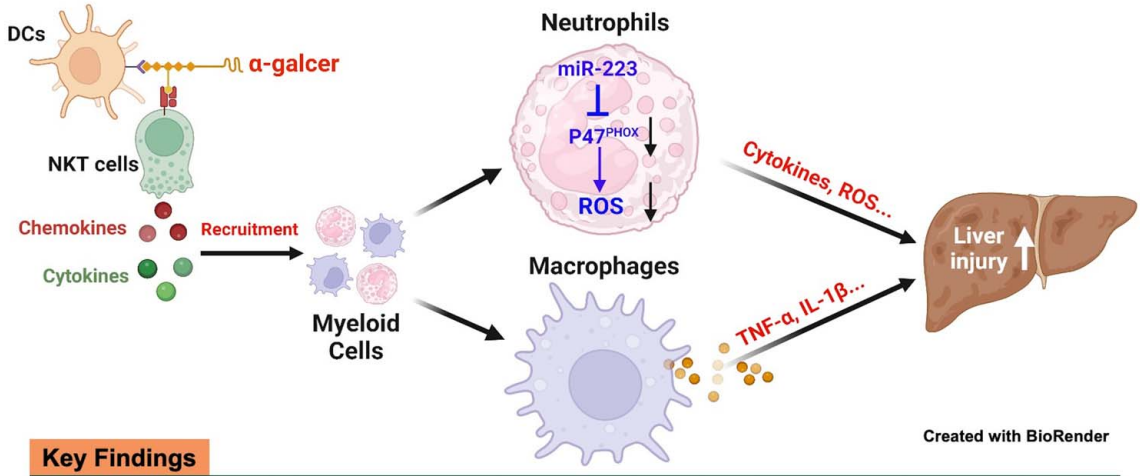

Key Findings

- Neutrophil and macrophage infiltration via multiple inflammatory mediators is required for NKT cell activation-induced hepatitis.
- Genetic deletion of neutrophil-specific miR-223 markedly enhances α-Galcer-induced NKT cell hepatitis.
- Neutrophil Cytosolic Factor 1 (*Ncf1*) deficiency significantly ameliorates liver inflammation and oxidative damage caused by α-Galcer.

Received: 16 July 2024 | Accepted: 27 September 2024

DOI: 10.1097/HC9.0000000000000592

ORIGINAL ARTICLE

OPEN

Multiple cell-type interactions drive invariant NKT cell hepatitis

Jiaxin Tan[1,2] | Longshan Ji[1,2] | Qian Li[1,2] | Ruowen Guo[1,2] | Yawen Hao[3,4] | Peng Xiao[5] | Qiuhong Zai[3,4] | Xuewei Zhang[6] | Yating Gao[1] | Xin Zhang[1,2] | Miao Fang[1,2] | Yanhang Gao[5] | Weidong Zhao[6] | Yong He[3,4] | Yueqiu Gao[1,2] | Man Li[1,2]

[1]Laboratory of Cellular Immunity, Shanghai Key Laboratory of Traditional Chinese Medicine, Shuguang Hospital Affiliated to Shanghai University of Traditional Chinese Medicine, Key Laboratory of Liver and Kidney Diseases (Shanghai University of Traditional Chinese Medicine), Ministry of Education, Shanghai, China

[2]Institute of Infectious Diseases of Integrated Traditional Chinese and Western Medicine, Shanghai Institute of Traditional Chinese Medicine, Shanghai, China

[3]Shanghai Institute of Materia Medica, Chinese Academy of Sciences, Shanghai, China

[4]University of Chinese Academy of Sciences, Beijing, China

[5]Department of Hepatology, First Hospital of Jilin University, Jilin University, Changchun, Jilin, China

[6]Department of Physiology, China Medical University, Shenyang, China

Correspondence
Yong He, Shanghai Institute of Materia Medica (SIMM), Chinese Academy of Sciences, 555 Zuchongzhi Road, Pudong, Shanghai 201203, China.
Email: heyong@simm.ac.cn

Man Li, Shuguang Hospital Affiliated to Shanghai University of Traditional Chinese Medicine, 528 Zhangheng Road, Pudong, Shanghai 201203, China.
Email: liman121000@shutcm.edu.cn

Yueqiu Gao, Shuguang Hospital Affiliated to Shanghai University of Traditional Chinese Medicine, 528 Zhangheng Road, Pudong, Shanghai 201203, China.
Email: gaoyueqiu@shutcm.edu.cn

Abstract

Background: α-Galactosylceramide (α-Galcer), a specific ligand for invariant natural killer T (NKT) cell activation, has been actively investigated in clinical trials such as antitumor therapy; however, treatment with α-Galcer is well known to induce acute hepatitis due to enriched NKT cells in the liver. The molecular mechanisms underlying NKT-mediated hepatitis still remain obscure. The object of this study was to investigate whether and how myeloid cells affect NKT-mediated hepatitis.

Methods: α-Galcer–induced NKT hepatitis was used in this study. microRNA-223 (miR-223) and neutrophil cytosolic factor 1 (*Ncf1*)–deficent mice were generated and subjected to α-Galcer–induced NKT hepatitis.

Results: In this study, we demonstrated that α-Galcer–induced NKT cell activation resulted in neutrophil and monocyte-derived macrophage accumulation in the liver. Importantly, serum levels of several hepatic myeloid cell infiltration–related cytokines and chemokines were significantly elevated after α-Galcer administration. Among these myeloid cells, blockade of neutrophil or macrophage migration through using different inhibitors of (C-X-C Motif) receptor 2, (C-C motif) receptor 2, and (C-C motif) receptor 5 signaling

Abbreviations: α-Galcer, α-Galactosylceramide; 4-HNE, 4-hydroxynonenal; CCR, C-C motif receptor; CXCR2, (C-X-C Motif) receptor 2; DCFH-DA, 2',7'-dichlorodihydro-fluorescein diacetate; IFN-γ, interferon γ; MCP-1, monocyte chemoattractant protein-1; MDA, malondialdehyde; MIP-1β, macrophage inflammatory protein 1-beta; miR-223, microRNA-223; NCF1, neutrophil cytosolic factor 1; NKT, natural killer T; ROS, reactive oxygen species; WT, wild-type.

Jiaxin Tan, Longshan Ji, and Qian Li contributed equally to this work.

ameliorated α-Galcer–induced liver injury, mainly due to the decrease of reactive oxygen species production and inflammation. Depletion of neutrophils reduced α-Galcer–induced liver injury and hepatitis. Interestingly, genetic deletion of neutrophil-specific miR-223 markedly enhanced while *Ncf1* deficiency significantly ameliorated liver inflammation and oxidative damage caused by α-Galcer.

Conclusions: Neutrophil and macrophage infiltration through multiple inflammatory mediators is required for NKT cell activation–induced hepatitis, which sheds light on the myeloid cell infiltration–related molecular mechanisms of NKT cell–mediated liver injury. Our study may provide a novel therapeutical strategy for the treatment of NKT cell hepatitis.

Keywords: inflammation, miR-223, myeloid cell, Ncf1, NKT cell, reactive oxygen species

INTRODUCTION

The disruption of liver immune cell homeostasis is one of the important reasons for immune-mediated liver injury.[1] Natural killer T (NKT) cells are an important component of immune cells and can not only express T-cell receptors but also have NK lineage markers.[2] It is well known that there are 2 main subsets of NKT cells: type I and type II NKT cells. Type I NKT cells, also known as invariant NKT cells, can rapidly produce various and large quantities of cytokines in response to stimuli, which link innate and adaptive immunity.[3] Type I invariant NKT cells exclusively express an invariant T-cell receptor-α chain, whereas type II NKT cells express more diverse T-cell receptors. The liver is an organ that has the largest amount of NKT cells, including 20%–35% and 10%–15% invariant NKT cells in mouse and human liver lymphocytes, respectively.[4] α-Galactosylceramide (α-Galcer), a natural molecule that was discovered in 1993, can specifically activate NKT cells to inhibit the development of tumors and has been actively investigated in clinical studies for the treatment of cancer.[5] Administration of α-Galcer induces hepatic injury, which has emerged as a robust model to investigate the fundamental pathophysiology of immune-mediated liver injury. However, the underlying mechanism by which α-Galcer causes liver injury remains unclear.

Bone marrow–derived myeloid cells, including neutrophils, monocytes, erythrocytes, and platelets, are accumulated in the liver during the development and progression of various liver diseases, including viral hepatitis, NAFLD, alcohol-associated liver disease, DILI, and HCC. Neutrophils were regarded as important participants in the inflammatory reaction through phagocytosis, degranulation, and extracellular traps (NETs).[6] Neutrophils also play critical roles in the pathogenesis of different kinds of liver diseases.[7,8] Neutrophils also improve liver inflammation and fibrosis in high-fat diet-feeding mice by transferring anti-inflammatory microRNA-223 (miR-223)-enriched extracellular vesicles to hepatocytes, finally inhibiting multiple inflammatory and oncogenic genes in hepatocytes.[9] In addition, neutrophils promote the conversion of proinflammatory Ly6C^{hi}CX3CR1^{lo} monocytes/macrophages to pro-resolving Ly6C^{lo}CX3CR1^{hi} macrophages through reactive oxygen species (ROS), which can accelerate the process of liver repair.[10] Interestingly, α-Galcer–mediated NKT hepatitis can cause the accumulation of neutrophils in the liver, leading to liver damage and inflammation.[11,12] Macrophages have complex roles in liver injury due to their diverse subsets: on the one hand, macrophages can accelerate liver inflammation in the early stages of liver injury,[13] and on the other hand, macrophages can promote liver regeneration in the late stages of liver injury.[14] KCs are the resident hepatic macrophages with potent phagocytic capacity, high density of surface scavenger, and pattern recognition receptors, and have the ability to release numerous mediators that govern the local immunological milieu.[15] However, whether and how myeloid cells, including neutrophils and monocyte-derived macrophages, contribute to α-Galcer–mediated liver injury remains obscure.

To define the functional roles of myeloid cells in α-Galcer–induced liver injury, we first measured serum levels of cytokines and chemokines after α-Galcer injection. Intriguingly, several hepatic myeloid cell infiltration–related cytokines and chemokines are elevated in α-Galcer–induced NKT cell hepatitis. Inhibition of neutrophil or monocyte migration ameliorates liver injury and inflammation. Neutrophils can damage the liver by mainly promoting ROS production as demonstrated that neutrophil-depleted are resistant to, anti-inflammatory

and anti-oxidative stress miR-223–deficient mice are more susceptible to, liver injury caused by α-Galcer. In contrast, neutrophil cytosolic factor 1 (NCF1)-deficient mice were more resistant to α-Galcer–induced liver injury by suppressing ROS production. Taken together, our study sheds light on the mechanisms of NKT cell–mediated liver injury, which may provide a novel therapeutical strategy for the treatment of liver injury.

METHODS

Mice

Six to 8-week-old C57BL/ 6J male mice, purchased from the center of experimental animals of Shanghai University of Traditional Chinese Medicine, were used in our study. Female miR-223 knockout mice (miR-223$^{-/-}$) (The Jackson Laboratory) were crossed with male C57BL/6J mice to obtain female miR-223$^{+/-}$ mice. Female miR-223$^{+/-}$ and male miR-223$^{-/y}$ mice (the miR-223 locus is on the X chromosome) were bred at the center of experimental animals of Shanghai University of Traditional Chinese Medicine to generate male miR-223$^{-/y}$ (male miR-223 knockout) and wild-type (WT) miR-223$^{+/y}$ littermate controls. All male miR-223$^{+/y}$ littermates were used as WT controls for male miR-223$^{-/y}$ mice in our study. The *P47$^{phox\ -/-}$* mice were generated as demonstrated in the previous paper.[16] The mice were i.v. injected with α-GalCer (150 μg/kg, Shanghai Yuanye biology, Cat No. 158021-47-7) to establish NKT cell–induced acute liver injury. For the neutrophil depletion experiment, 150 μg of either RB6-8C5 (Ly-6G/Ly-6C Monoclonal Antibody; Invitrogen; Cat No. 14-5931-82) or isotype control Ab (Rat IgG2a; Invitrogen; Cat No. 14-4031-82) was injected (i.v.) 4 hours before α-Galcer treatment. To inhibit different receptor-mediated signaling, the mice were treated with CXCR2 (C-X-C Motif receptor 2) inhibitor AZD5069 (10 mg/kg, MCE, Cat No. HY-19855) at 3 hours before α-Galcer treatment. Rs5043939 (5 mg/kg, MCE, Cat No. HY-15418) and Maraviroc (10 mg/kg, MCE, Cat No. HY-13004) were administrated to inhibit C-C motif receptor (CCR)2 or CCR5 signaling in mice at 30 minutes before α-Galcer treatment. Liver samples were collected 16 hours after α-Galcer injection. All animal experiments were approved by the Committee of Animal Experimentation and conducted at Shanghai University of Traditional Chinese Medicine in accordance with its Animal Experiment Guidelines.

Total RNA isolation and reverse transcription-quantitative PCR

Total RNA was extracted from liver tissues and neutrophils by using the RNAiso Plus reagent (cat number: RP4002; Biotech). One thousand nanograms of total RNA were reverse-transcribed with the Hiscript II Reverse Transcriptase Kit (cat number: R223-01; Vazyme Biotech). The relative expression levels of genes were measured by ChamQ SYBR qPCR Master Mix (cat number: Q311-02; Vazyme Biotech) and detected by CFX96 Thermal Cycler (Bio-Rad). The primer sequences are included in Table 1.

Histologic analysis

Liver tissues fixed by 4% paraformaldehyde were embedded in paraffin and cut at 5 μm thickness. The sections were subjected to hematoxylin-eosin staining according to the manufacturer's protocol. For immunohistochemistry, after heat-induced epitope retrieval, the sections were incubated in 3% H_2O_2 and blocked for another 60 minutes in 3% normal goat serum buffer. Sections were incubated with primary antibodies overnight at 4 °C. The SignalStain Boost IHC detection reagent (HRP, Rabbit or mouse) (Cell Signaling Technology) was performed for 35 minutes at RT. DAB Peroxidase Substrate Kit (Vector Laboratories, Inc.) was used to visualize the staining according to the manufacturer's instructions. Antibodies used in immunohistochemistry staining included MPO (Cat No. APR 023AA, H; Biocare Medical), Ly6G (Cat No.87048S, CST), F4/80 (Cat No.70076S, CST), malondialdehyde (MDA) (Cat No.MMD-030n, Jiaca), and 4-hydroxynonenal (4-HNE) (Cat No.MHN-100P, Jiaca).

For immunofluorescence staining, after primary antibody incubation overnight, the Alexa Fluor–conjugated secondary antibody such as Alexa Fluor 488 goat anti-rabbit IgG (H+L) (Cat No. 4412S, CST), Alexa Fluor 555 goat anti-Rat IgG (H+L) (Cat No. 4417S, CST) were incubated for 1 hour at room temperature. Slides were incubated with 1 mg/mL DAPI for 5 minutes for nuclear staining. The images were obtained by using OLYMPUS APEXVIEW APX100 with filters allowing the detection of Alexa Fluor 488 and 555. The antibodies against IBA-1 or CLEC4F were purchased from Cell Signaling Technology (Cat No.17098S) and R&D Systems (Cat No. MAB2784), respectively.

Neutrophil isolation

Neutrophils were isolated from liver tissues by using the Neutrophil Isolation Kit (Cat No. 130-097-658; Miltenyi Biotec). In brief, nontarget cells were indirectly magnetically labeled with a cocktail of biotin-conjugated monoclonal antibodies as primary labeling reagent and anti-biotin monoclonal antibodies conjugated to MicroBeads, as secondary labeling reagent. The magnetically labeled nontarget cells were depleted by retaining them within a MACS Column in the magnetic field of a MACS Separator, while the unlabeled neutrophils through the column were collected.

TABLE 1 RT-qPCR primer sequences

Mouse-IL-6-Forward	TCCATCCAGTTGCCTTCTTG
Mouse-IL-6-Reverse	TTCCACGATTTCCCAGAGAAC
Mouse-IL-1β-Forward	TCGCTCAGGGTCACAAGAAA
Mouse-IL-1β-Reverse	CATCAGAGGCAAGGAGGAAAAC
Mouse-TNF-α-Forward	AGGCTGCCCCGACTACGT
Mouse-TNF-α-Reverse	GACTTTCTCCTGGTATGAGATAGCAAA
Mouse-IFN-γ-Forward	ATGAACGCTACACACTGCATC
Mouse-IFN-γ-Reverse	CCATCCTTTTGCCAGTTCCTC
Mouse-P47^{phox}-Forward	TCCTCTTCAACAGCAGCGTA
Mouse-P47^{phox}-Reverse	CTATCTGGAGCCCCTTGACA
Mouse-P67^{phox}-Forward	TCTATCAGCTGGTTCCCACG
Mouse-P67^{phox}-Reverse	TGGCCTACTTCCAGAGAGGA
Mouse-P40^{phox}-Forward	ATCGTCTGGAAGCTGCTCAA
Mouse-P40^{phox}-Reverse	CCCATCCATCTGCTTTTCTG
Mouse-gp91^{phox}-Forward	GACCATTGCAAGTGAACACCC
Mouse-gp91^{phox}-Reverse	AAATGAAGTGGACTCCACGCG
Mouse-P22^{phox}-Forward	ATGGAGCGATGTGGACAGAAG
Mouse-P22^{phox}-Reverse	TAGATCACACTGGCAATGGCC
Mouse-CCL2-Forward	TTAAAAACCTGGATCGGAACCAA
Mouse-CCL2-Reverse	GCATTAGCTTCAGATTTACGGGT
Mouse-CXCL2-Forward	TCCAGGTCAGTTAGCCTTGC
Mouse-CXCL2-Reverse	CGGTCAAAAAGTTTGCCTTG
Mouse-CXCL10-Forward	CCAAGTGCTGCCGTCATTTTC
Mouse-CXCL10-Reverse	GGCTCGCAGGGATGATTTCAA
Mouse-CXCL11-Forward	GGCTTCCTTATGTTCAAACAGGG
Mouse-CXCL11-Reverse	GCCGTTACTCGGGTAAATTACA

Abbreviations: IFN-γ, interferon γ; RT-qPCR, reverse transcription-quantitative polymerase chain reaction.

Measurement of ROS, 4-HNE, and MDA

The levels of ROS were detected using fluorescent probe 2',7'-dichloro-dihydro-fluorescein diacetate (DCFH-DA, Nanjing Jian Cheng Bioengineering Institute). Neutrophils were collected and incubated with DCFH-DA for 30 minutes at 37 °C in the dark. Next, the fluorescence intensity was measured using flow cytometry (Beckman Coulter).

The levels of 4-HNE in liver tissue were measured by using an ELISA kit (Nanjing Jian Cheng, Cat No. A003-1-2) according to the manufacturer's protocols. The MDA assay kit (Cat No. H268-1-2) was purchased from Nanjing Jian Cheng Bioengineering Research Institute. All kit assays were performed following the manufacturer's protocol.

Flow cytometric analysis

The liver tissues were minced and tamped through the 70-mm nylon mesh. Liver leukocytes were purified by centrifugation on the Percoll gradient, and the remaining red blood cells were lysed by red blood cell lysis buffer (Cat No. 00-4333-57; eBioscience). Neutrophils were detected by antibodies against mouse CD45-Percp (Cat No. 103130; BioLegend), Gr-1-PE (Cat No. 127608; BioLegend), and CD11b-FITC (Cat No. 101206; BioLegend). Flow cytometric analysis was performed according to standard settings on a CytoFLEX flow cytometer (Beckman Coulter) and analyzed with Flowjo software (Treestar).

The detection of serum cytokines and chemokines

The serum cytokines or chemokines were detected respectively using a LEGENDplex kit (Cat No. B227962 and Cat No. B231031; BioLegend), according to the manufacturer's instructions. In a nutshell, LEGENDplex is a microbead-based immunoassay method, and its principle is consistent with the classic "sandwich" Immunoassay method. Each microbead is coupled with a capture antibody corresponding to the corresponding indicator, which can specifically capture the target protein (analyte) in the sample or standard. Capturing microbeads, the target analyte, and the added detection

antibody form a double antibody "sandwich" structure, which reacts with Streptavidin-PE (SA-PE) after incubation and washed. Then flow cytometry detects the fluorescence signal intensity of each group of microbeads to reflect the numbers of the analyte. Finally, for quantitative analysis, LEGENDplex Data Analysis V8.0 was used, following the manufacturer's recommended protocols.

RNA sequencing

Total RNA was isolated using the Trizol Reagent (Invitrogen Life Technologies), after which the concentration, quality, and integrity were determined using a NanoDrop spectrophotometer (Thermo Scientific). Three micrograms of RNA were used as input material for the RNA sample preparations. Sequencing libraries were generated according to the following steps. First, mRNA was purified from total RNA using poly-T oligo-attached magnetic beads. Fragmentation was carried out using divalent cations under elevated temperature in an Illumina proprietary fragmentation buffer. First-strand cDNA was synthesized using random oligonucleotides and Super Script II. Second-strand cDNA synthesis was subsequently performed using DNA Polymerase I and RNase H. Remaining overhangs were converted into blunt ends through exonuclease/polymerase activities, and the enzymes were removed. After adenylation of the 3′ ends of the DNA fragments, Illumina PE adapter oligonucleotides were ligated to prepare for hybridization. To select cDNA fragments of the preferred 400–500 bp in length, the library fragments were purified using the AMPure XP system (Beckman Coulter). DNA fragments with ligated adaptor molecules on both ends were selectively enriched using Illumina PCR Primer Cocktail in a 15-cycle PCR reaction. Products were purified (AMPure XP system) and quantified using the Agilent high-sensitivity DNA assay on a Bioanalyzer 2100 system (Agilent). The sequencing library was then sequenced on the NovaSeq 6000 platform (Illumina; Shanghai Personal Biotechnology Co. Ltd.). Full RNAseq data have been uploaded to NCBI Sequence Read Archive (SRA) (The SRA number is SRP568908).

Statistical analysis

Data are expressed as the means ± SEM and were analyzed by 2-tailed unpaired Student *t* test using GraphPad Prism software (v. 9.0a; GraphPad Software). To compare values obtained from the 2 groups, the Student *t* test was performed. Data from multiple groups were compared with 1-way ANOVA followed by the Tukey post hoc test. p values of < 0.05 were considered significant.

RESULTS

α-Galcer–induced NKT hepatitis is associated with accumulation of neutrophils and infiltrated macrophages

Previous studies have reported that the specific activation of NKT cells caused by α-Galcer leads to liver injury and inflammation.[11] Herein, we demonstrated that after α-Galcer injection, serum ALT and AST levels were continuously elevated, peaking at 16 hours and decreasing at 24 hours (Figure 1A). Consistently, hematoxylin-eosin staining showed that inflammatory cells were infiltrated in the liver after α-Galcer injection (Figure 1B). To understand the molecular mechanisms by which activation of NKT cells induces liver injury, we examined the hepatic infiltration of neutrophils and macrophages. As illustrated in Figure 1C, MPO^+ neutrophils and F4/80+ macrophages were significantly increased in the liver after α-Galcer injection (Figure 1C). Next, we performed the double dual immunofluorescence staining results to distinguish liver resident macrophages (KCs, $IBA1^+$-$CLEC4F^+$) and infiltrating macrophages ($IBA1^+CLEC4F^{-}$). The results revealed that these macrophages are monocyte-derived macrophages (Figure 1D).

Disorder of serum cytokines and chemokines after α-Galcer treatment

To investigate the mechanism by which α-Galcer injection promotes liver neutrophil and macrophage accumulation, we analyzed the changes in serum cytokines and chemokines at different time points after α-Galcer treatment. As shown in Figure 2A, serum interferon γ (IFN-γ), IL-2, and IL-4 were the 3 most significant elevated cytokines among all detected cytokines. Several other cytokines were also elevated after α-Galcer treatment. Among them, IFN-γ and IL-5 reached their peaks at 16 hours and then began to decline; IL-2, IL-4, TNF-α, IL-6, IL-13, IL-17A, and IL-22 reached their peaks at 3 hours and then returned to basal levels at 9–16 hours (Figure 2A). Next, we measured serum chemokine levels after α-Galcer injection. As shown in Figure 2B, the levels of CXCL1 (C-X-C motif chemokine ligand 1) showed the most significant change among all detected chemokines. CXCL1, MCP-1 (monocyte chemoattractant protein-1), MIP-1β (macrophage inflammatory protein 1-beta), MIP-1α, and IP-10 (10 kDa interferon gamma-induced protein, C-X-C motif chemokine ligand 10) reached their peak at early time point (3 h) and then began to return to basal levels; however, RANTES (regulation of activation, expression and secretion by normal T cells, C-C motif chemokine ligand 5), MIG (C-X-C motif chemokine ligand 9), Eotaxin (C-C motif chemokine ligand 11), BLC (C-X-C motif chemokine ligand 13),

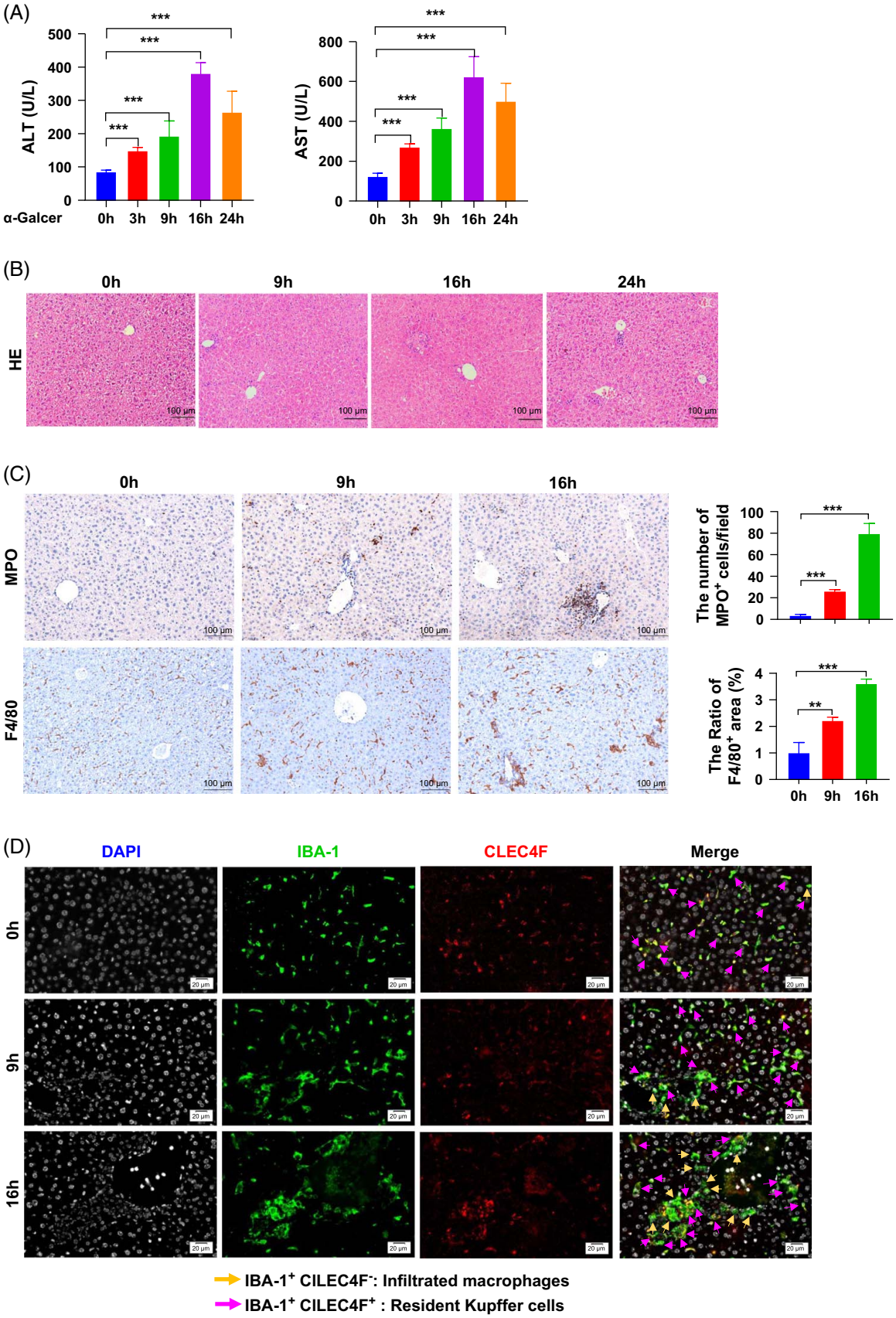

FIGURE 1 α-Galcer–induced invariant NKT cell activation leads to hepatic myeloid cell infiltration. C57BL/6J mice (n = 5) were injected with α-Galcer through tail vein injection (150 μg/kg). Serum and liver tissue samples were collected. (A) The levels of serum ALT and AST at different time

points after α-Galcer treatment were measured. (B) The degree of inflammatory cell infiltration in the liver at different time points after α-Galcer treatment was analyzed by H&E staining. (C) Liver tissues were subjected to MPO and F4/80 immunostaining, and the quantitation of MPO^+ and $F4/80^+$ cells per field was determined. Representative images are shown. (D) The infiltrated MoMFs were increased at different time points after α-Galcer treatment, which is distinguished by dual immunofluorescence staining ($IBA\text{-}1^+$ $CLEC4F^-$: infiltrated macrophages; $IBA\text{-}1^+$ $CLEC4F^+$: resident KCs). Values represent means ± SD. $^{**}p < 0.01$, $^{***}p < 0.001$. Abbreviations: α-Galcer, α-Galactosylceramide; H&E, hematoxylin-eosin; MoMF, monocyte-derived macrophages; NKT, Natural killer T.

MDC (C-C motif chemokine ligand 22), and TARC (C-C motif chemokine ligand 17) reached their peak at later time point (9 h) and then began to decline. Interestingly, the levels of LIX (C-X-C motif chemokine ligand 5) were slightly decreased after α-Galcer treatment (Figure 2B). Upregulation of these chemokines likely contributes to hepatic infiltration of neutrophils and macrophages in α-Galcer–induced hepatitis.

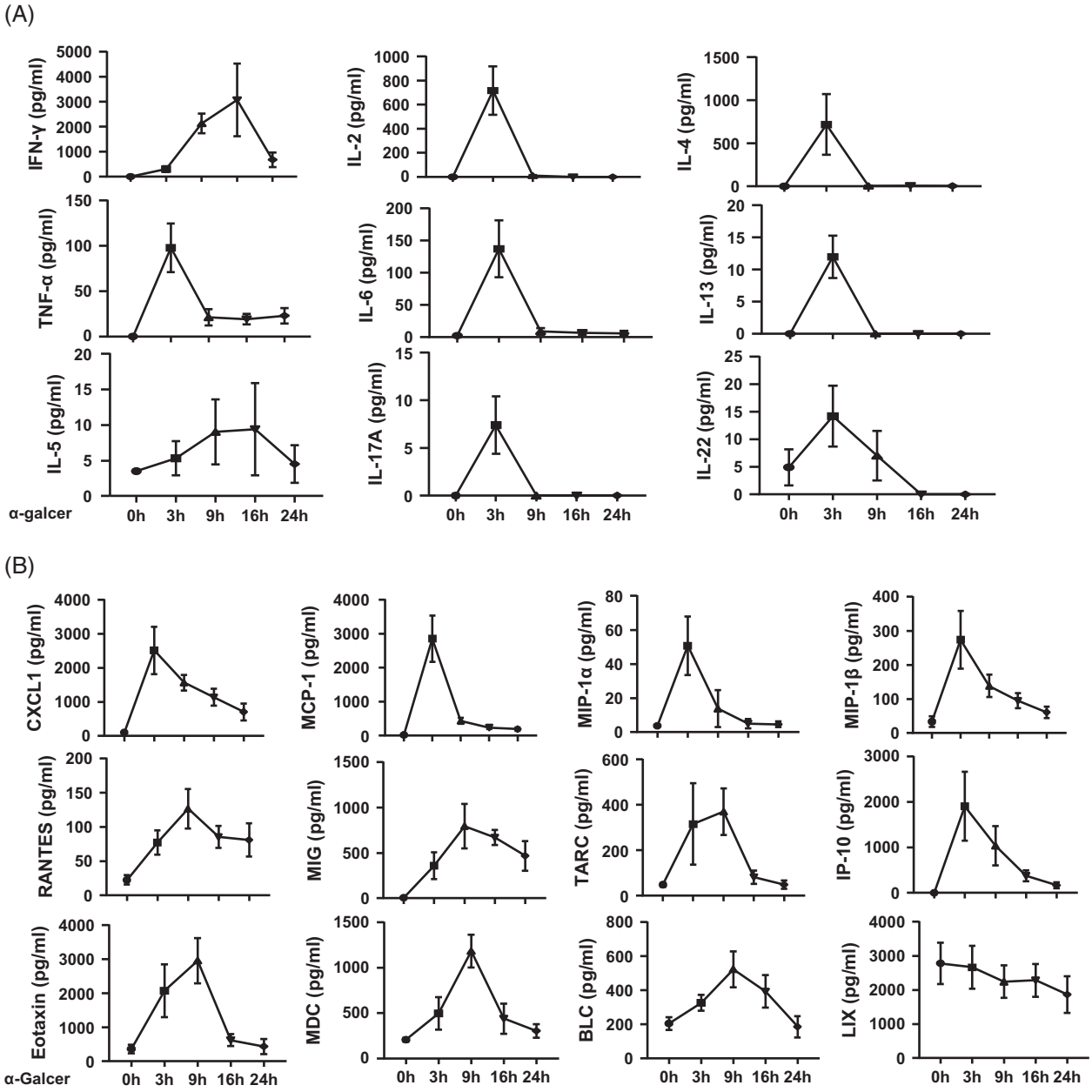

FIGURE 2 Disorder of serum cytokines and chemokines after α-Galcer treatment. The mice were injected with α-Galcer as described in Figure 1. Serum and liver tissue samples were collected. (A) The levels of serum cytokines at different time points after α-Galcer treatment, such as IFN-γ, IL-2, IL-4, TNF-α, IL-6, IL-13, IL-5, IL-17A, and IL-22, were measured. (B) The expressions of serum chemokines at different time points after α-Galcer treatment, including CXCL1, MCP-1, MIP-α, MIP-β, RANTES (CCL5), MIG (CXCL9), TRAC (CCL17), IP-10 (CXCL10), Eotaxin (CCL11), MDC (CCL22), BLC (CXCL13), LIX (CXCL5), were measured. Abbreviations: α-Galcer, α-Galactosylceramide; IFN-γ, interferon γ.

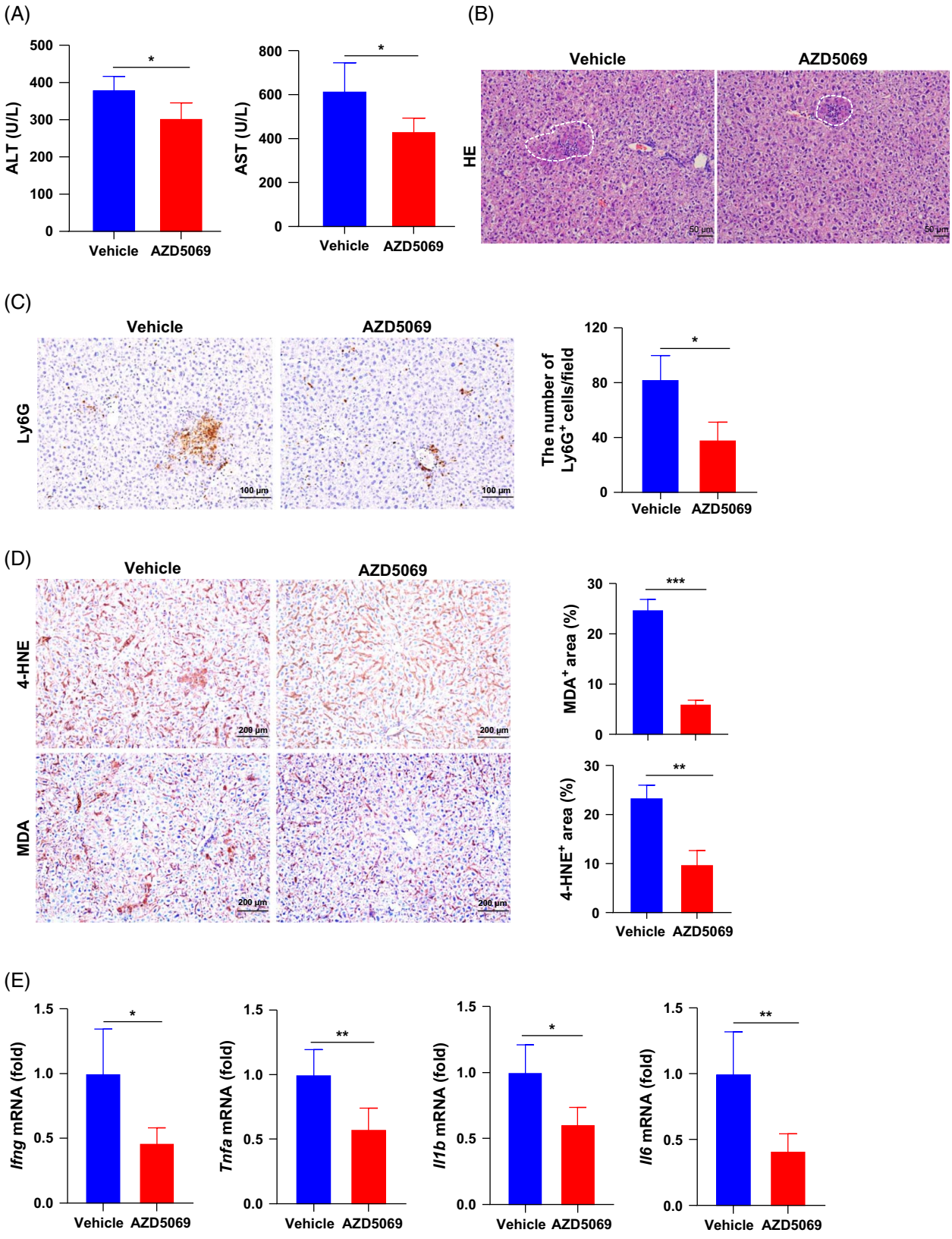

FIGURE 3 CXCR2 signaling inhibitor reduces α-Galcer–induced neutrophil accumulation, thus ameliorating liver injury. The mice were injected with CXCR2 signaling inhibitor AZD5069 or vehicle 3 hours before α-Galcer treatment. Serum and liver tissue samples were collected after α-Galcer treatment for 16 hours. (A) The levels of ALT and AST in serum were measured. (B) The degree of inflammatory cell infiltration in the liver was analyzed by H&E staining. (C) Liver tissues were subjected to MPO immunostaining, and the quantitation of MPO^+ cells per field was determined. Representative images are shown. (D) The levels of MDA and 4-HNE were determined by immunohistochemical staining.

Representative images are shown. The quantitation of MDA$^+$ and 4-HNE$^+$ area per field was determined. (E) The mRNA expression of several genes in the liver, including IFN-γ, TNF-α, IL-1β, and IL-6, were analyzed by RT-qPCR. Values represent means ± SD. *$p < 0.05$, **$p < 0.01$, ***$p < 0.001$. Abbreviations: α-Galcer, α-Galactosylceramide; 4-HNE, 4-hydroxynonenal; H&E, hematoxylin-eosin; IFN-γ, interferon γ; MDA, malondialdehyde; RT-qPCR, reverse transcription-quantitative polymerase chain reaction.

Blocking the CXCL1-CXCR2 axis can effectively inhibit neutrophil infiltration, and ameliorate α-Galcer–induced liver injury

Given that CXCL1, a major chemokine for neutrophil chemotaxis, is one of the most highly upregulated chemokines in α-Galcer–induced hepatitis, we wondered whether CXCL1 is involved in α-Galcer–induced liver injury. We used AZD5069 (an inhibitor of CXCR2, which is the receptor for CXCL1) to block the CXCL1-CXCR2 axis. As shown in Figures 3A and B, compared with the vehicle group, serum levels of ALT and AST in the CXCR2 inhibitor–treated group were significantly lower, and fewer inflammatory cell infiltrates were observed in the liver. The infiltration of neutrophils in the liver is reduced considerably (Figure 3C). In addition, we also found the accumulation of MDA and 4-HNE was also reduced compared with the vehicle group (Figure 3D). The expressions of *Ifng*, *Tnfa*, *Il1b*, and *Il6* mRNA in the CXCR2 inhibitor–treated group were remarkedly decreased compared with the vehicle group after α-Galcer injection (Figure 3E).

Neutrophil-derived oxidative stress leads to α-Galcer–induced liver damage

To investigate whether neutrophil-derived ROS contribute to α-Galcer–induced hepatitis, we measured ROS produced by neutrophils. The flow cytometry results showed that neutrophils-derived ROS was greater in the α-Galcer–treated group than in the vehicle group (Figure 4A). Besides, α-Galcer treatment promoted the accumulation of hepatic oxidative stress–related adducts, including MDA and 4-HNE (Figures 4B, C). Moreover, we used an anti-Ly6G antibody to deplete neutrophils, which was confirmed by immunohistochemistry analysis of MPO (Figure 4D). Depletion of neutrophils remarkedly lowered serum levels of ALT and AST compared with the isotype antibody group (Figure 4E). Importantly, the accumulation of Inflammatory cells and MDA and 4-HNE levels were significantly suppressed after Ly6G antibody treatment (Figures 4F–H) as well as by CXCR2 inhibitor treatment.

Inhibiting CCR2 or CCR5 signaling alleviates α-Galcer–induced liver injury, neutrophil infiltration, and ROS production

Given the dysregulation of several chemokines for macrophage chemotaxis, it is noteworthy to investigate the function of macrophages in α-Galcer–induced liver injury. RS504393 is a selective CCR2 chemokine receptor antagonist and can inhibit MCP-1–induced chemotaxis. Maraviroc is a selective CCR5 antagonist and can inhibit MIP-1β or RANTES-induced chemotaxis. Next, we used 2 antagonists, RS504393 and Maraviroc, respectively, in this study due to high elevation of serum MCP-1, MIP-1β, and RANTES after α-Galcer injection. Our results showed that α-Galcer–induced elevation of serum ALT and AST was reduced by CCR2 antagonist or CCR5 antagonist (Figure 5A). There was also less infiltration of macrophages and neutrophils in the liver after CCR2 antagonist or CCR5 antagonist administration in the α-Galcer–treated liver injury model (Figures 5B–E). Interestingly, α-Galcer–induced elevation of neutrophil-derived ROS was obviously reduced by CCR2 antagonist or CCR5 antagonist (Figure 5F). As expected, CCR2 antagonist or CCR5 antagonist administration lowered the hepatic accumulation of MDA or 4-HNE and the expression levels of hepatic *Ifng*, *Tnfa*, *Il1b*, and *Il6* mRNA (Figures 5F, G, and I). These results indicate that inhibiting CCR2 or CCR5 signaling can alleviate α-Galcer–induced liver injury.

P47^{phox}-mediated ROS production exacerbates α-Galcer–induced hepatitis

To understand the mechanisms underlying by which neutrophil-derived ROS production is increased after α-Galcer treatment, we examined the mRNA expression of NADPH-associated molecules in liver neutrophils isolated from α-Galcer–treated mice, which consisted of 5 phagocytic oxidases (phox) units: *p47^{phox}* (*Ncf1*), *p67^{phx}* (*Ncf2*), *p40^{phox}* (*Ncf4*), *p22^{phox}*, and *gp91^{phox}*. As shown in Figure 6A, *p47^{phox}* mRNA was significantly elevated in the model group, but other genes (*p67^{phox}*, *p40^{phox}*, *p22^{phox}*, and *gp91^{phox}*) were not altered or significantly decreased. Next, to better understand the functional role of *p47^{phox}* in α-Galcer–induced hepatitis, *P47^{phox}* knockout (*P47$^{phox-/-}$*) mice were generated. Interestingly, compared to WT mice, serum ALT and AST levels in *P47$^{phox-/-}$* mice were significantly reduced after α-Galcer treatment (Figure 6B). In addition, *P47$^{phox-/-}$* mice had less infiltration of inflammatory cells, such as MPO$^+$ neutrophils (Figure 6C). Compared with WT mice, the expression levels of MDA in the liver of *P47$^{phox-/-}$* mice were decreased, but the expression levels of 4-HNE remained unchanged (Figure 6D). To understand how P47^{phox} exacerbates α-Galcer–induced liver injury, we performed RNA sequencing on the liver

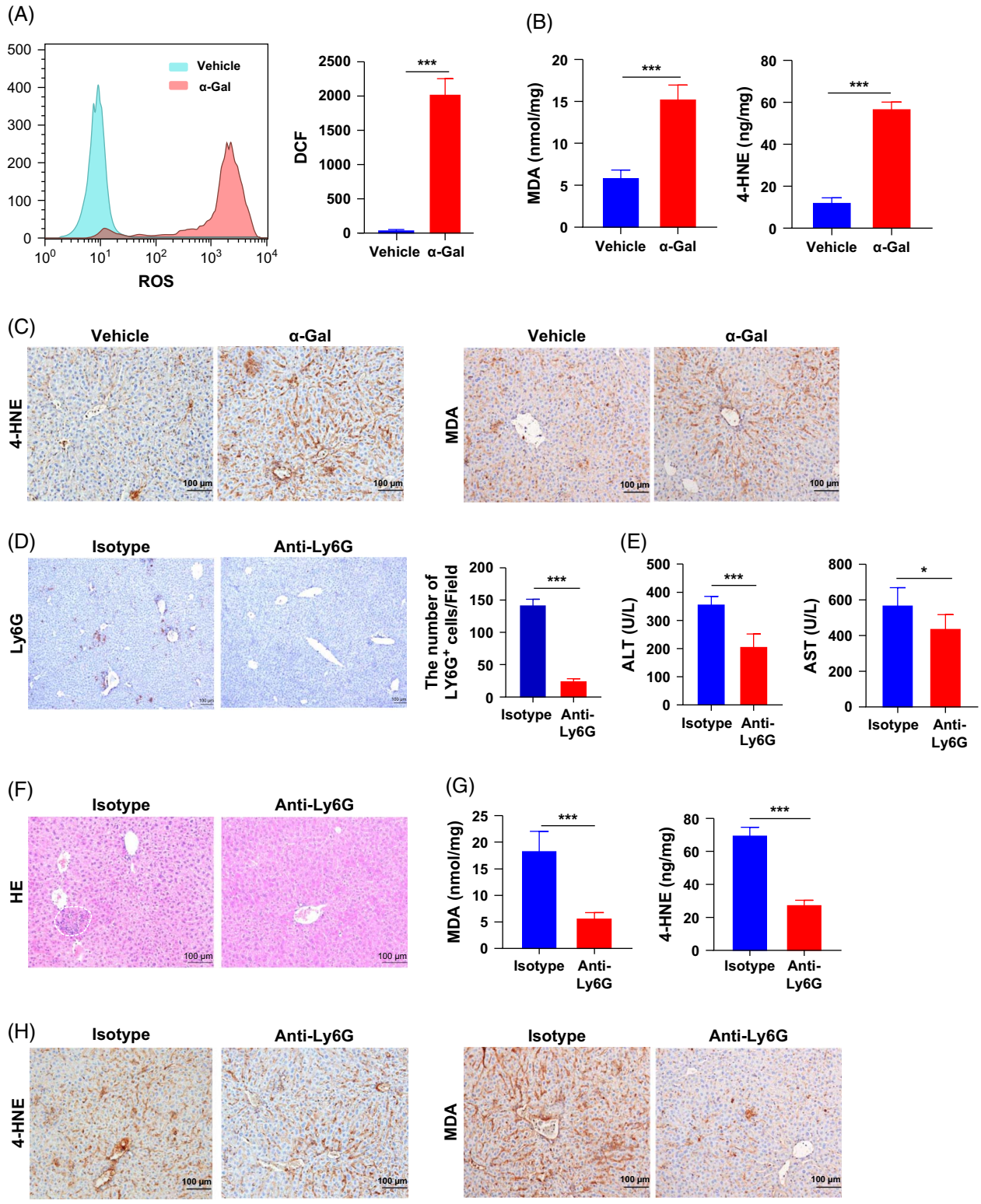

FIGURE 4 Neutrophil-derived oxidative stress contributes to α-Galcer–induced liver damage. The mice were injected with α-Galcer as described in Figure 1. Serum and liver tissue samples were collected after α-Galcer treatment for 16 hours. (A) The levels of ROS in neutrophils from the liver were analyzed by flow cytometry. (B, C) The hepatic levels of MDA and 4-HNE were analyzed by Elisa assay and IHC staining. (D) The mice were injected with an isotype antibody or anti-Ly6G antibody 4 hours before α-Galcer treatment. Serum and liver tissue samples were collected after α-Galcer treatment for 16 hours. The depletion of neutrophils in the liver was confirmed by immunostaining of Ly6G. (E) The levels of ALT and AST in serum were measured. (F) Hepatic inflammatory cell infiltration was analyzed by H&E staining. (G, H) The hepatic levels of MDA and 4-HNE in isotype or anti-Ly6G antibody-treated mice were analyzed by Elisa assay and IHC staining. Values represent means ± SD. *$p < 0.05$, ***$p < 0.001$. Abbreviations: α-Galcer, α-Galactosylceramide; 4-HNE, 4-hydroxynonenal; H&E, hematoxylin-eosin; IHC, immunohistochemistry; MDA, malondialdehyde; ROS, reactive oxygen species.

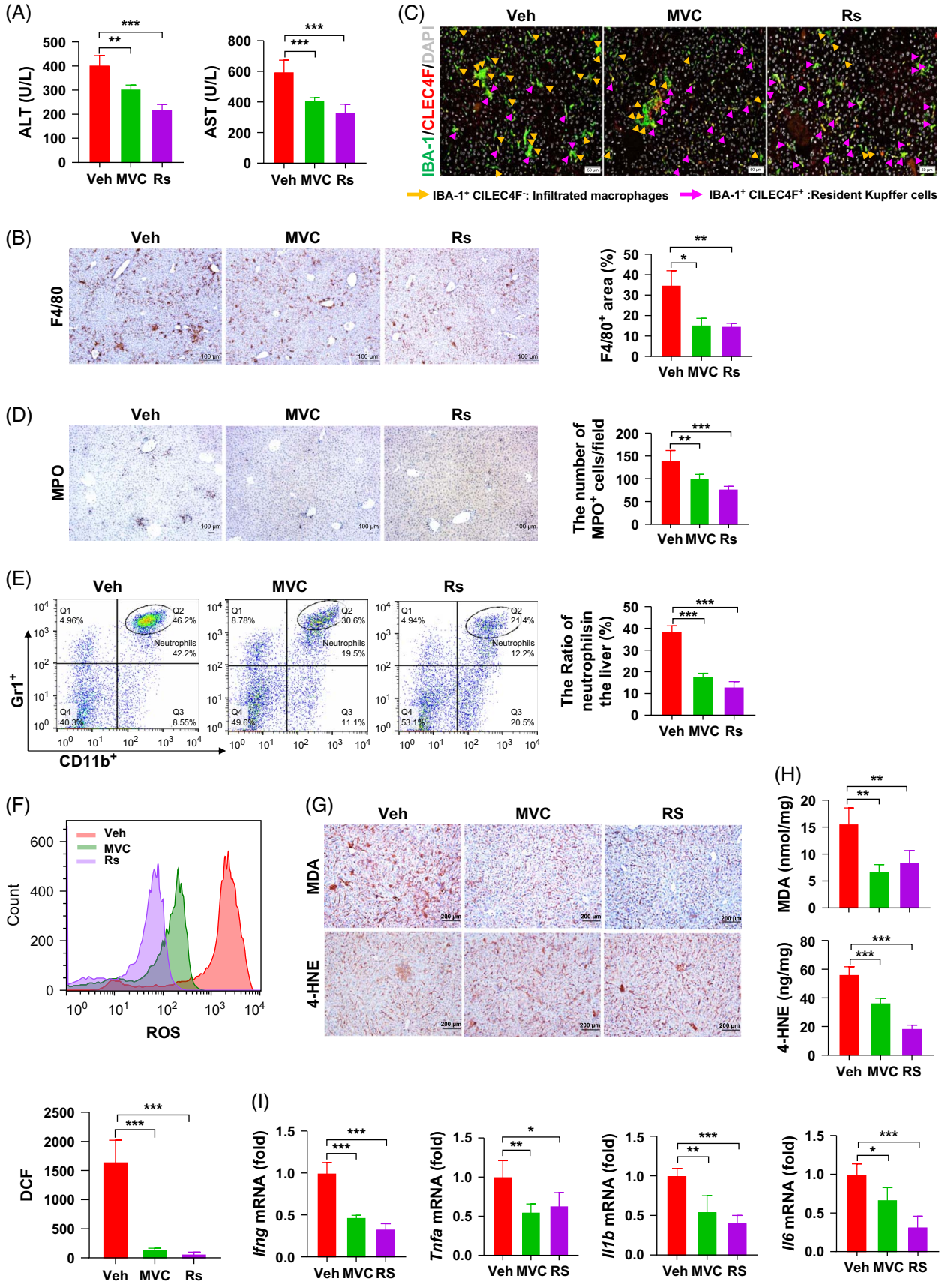

FIGURE 5 Inhibiting CCR2 or CCR5 signaling can alleviate liver injury caused by α-Galcer. Mice were treated with α-Galcer for 16 hours, and the CCR2 or CCR5 inhibitors were injected 30 minutes before α-Galcer treatment. Serum and liver tissue samples were collected after α-Galcer

treatment for 16 hours. (A) The levels of ALT and AST in serum were measured. (B) F4/80$^+$ macrophages were measured by immunohistochemical staining. (C) Identification of infiltrating macrophages and Resident Kcs in the liver by immunofluorescence staining. (D, E) MPO$^+$ and CD45$^+$CD11b$^+$Gr1$^+$ neutrophils were examined by immunohistochemical staining and flow cytometry, respectively. (F) The levels of ROS in neutrophils were analyzed. (G, H) The hepatic levels of MDA and 4-HNE in vehicle or inhibitor-treated mice were analyzed by IHC staining and Elisa assay. (I) The hepatic expression of inflammation-related genes, such as IFN-γ, TNF-α, IL-1β, and IL-6, were analyzed by RT-qPCR. Values represent means ± SD. *$p < 0.05$, **$p < 0.01$, ***$p < 0.001$. Abbreviations: α-Galcer, α-Galactosylceramide; 4-HNE, 4-hydroxynonenal; CCR2, C-C motif chemokine receptor 2; CCR5, C-C motif chemokine receptor 5; IFN-γ, interferon γ; IHC, immunohistochemistry; MDA, malondialdehyde; ROS, reactive oxygen species; RT-qPCR, reverse transcription-quantitative polymerase chain reaction.

tissues of WT and *P47$^{phox-/-}$* mice. The GO enrichment analysis showed that the differentially expressed genes' biological process (BP) are related to inflammatory responses and immune responses; the differentially expressed genes' molecular function (MF) included cytokine activity, receptor-ligand activity, and so on; and the differentially expressed genes' cellular components included the extracellular space, cell surface, etc (Figure 6E). Among these 20 genes (ranked by *p* value) with the most significant decrease in *P47$^{phox-/-}$* mice, chemokines such as *Ccl2*, *Cxcl2*, *Cxcl10*, and *Cxcl11* were included (Figure 6F). Indeed, we confirmed that compared with WT mice, the mRNA levels of *Ccl2*, *Cxcl2*, *Cxcl10*, and *Cxcl11* were lower in *P47$^{phox-/-}$* mice after α-Galcer treatment (Figure 6G). These results strongly indicate that neutrophils produce greater ROS through elevating P47^{phox}, thus exacerbating α-Galcer–induced liver injury.

Neutrophil-specific miR-223 acts as a negative feedback that inhibits α-Galcer–induced neutrophil-derived ROS and liver injury

Accumulating studies demonstrated that miRNA-223, a highly neutrophil-specific miRNA, is well-known to limit neutrophil activation and chemotaxis[17] and inhibit P47^{phox} expression in neutrophils. To investigate whether miR-223 is involved in α-Galcer–induced neutrophil ROS production and liver injury, we first measured hepatic miR-223 expression in α-Galcer–induced liver injury. As shown in Figure 7A, miR-223 was prominently upregulated in the liver after α-Galcer treatment for 16 hours. To study the function of miR-223 in α-Galcer–induced liver injury, we used miR-223$^{-/Y}$ mice. As illustrated in Figures 7B, C, miR-223$^{-/Y}$ mice were more susceptible to α-Galcer–induced liver injury as evidenced by higher serum levels of ALT, AST, and the greater degree of inflammatory cell infiltration compared with wild-type (WT) mice. In addition, hepatic expressions of 4-HNE and MDA in miR-223$^{-/Y}$ mice were higher than those in WT mice (Figure 7D). These results revealed that the absence of miR-223 exacerbated ROS production and liver damage after α-Galcer treatment, suggesting that miR-223 forms a negative feedback to prevent α-Galcer–induced neutrophil ROS production and liver injury.

DISCUSSION

The antitumor function of α-Galcer and NKT cells has been suggested in the past 20 years.[18,19] The product of NKT cell therapy "GKL-006" has been approved to be used in clinical trials by China's Center for Drug Evaluation in 2023. However, the remarkable enrichment of NKT cells in livers has attracted much research attention to investigate the functional role of this unique cell population in the pathophysiology of several liver diseases. Importantly, the question of why α-Galcer induces NKT production of a wide variety of cytokines and chemokines urgently needs to be addressed before the application of α-Galcer in additional clinical trials for treating liver disease. Although previous studies have provided a detailed review of the role of NKT cell activation in various liver diseases such as alcohol-associated liver disease, nonalcoholic liver disease, autoimmune hepatitis, HBV, HCV, and HCC,[20] the mechanism of NKT cell–induced liver injury remains obscure. In this study, we provided several key findings demonstrating that hepatic myeloid cell infiltration is involved in NKT cell–mediated hepatitis. First, we found that myeloid cell infiltration–related cytokines and chemokines are dysregulated after α-Galcer injection. Second, neutrophil-derived ROS contributes to immune-mediated liver injury, and neutrophil-specific miR-223 plays a key role in the development of α-Galcer–induced hepatitis by limiting ROS production and inflammation. Finally, we also found that chemokine-induced infiltration of monocyte macrophages during α-Galcer–induced liver injury (Figure 8).

The first striking finding from the current study is the significant changes of the cytokines after NKT cell activation. As we know, IFN-γ and IL-4 are 2 major cytokines secreted by NKT cells. IFN-γ can inhibit virus replication and reduce survival; however, it can induce inflammation by promoting polarization of macrophages to an M1 proinflammatory phenotype.[21] Interestingly, Wang et al[12] found that an absence of IFN-γ not only can not reduce the liver injury caused by NKT cells activation but also lead to a more serious injury, suggesting that the IFN-γ is not the main reason for α-Galcer–induced liver injury. We also found that IL-2 is rapidly increased in serum, and this may be related to the function of IL-2, which can promote the proliferation and differentiation of lymphocytes. It has been reported that NKT cells are able to expand after the combined

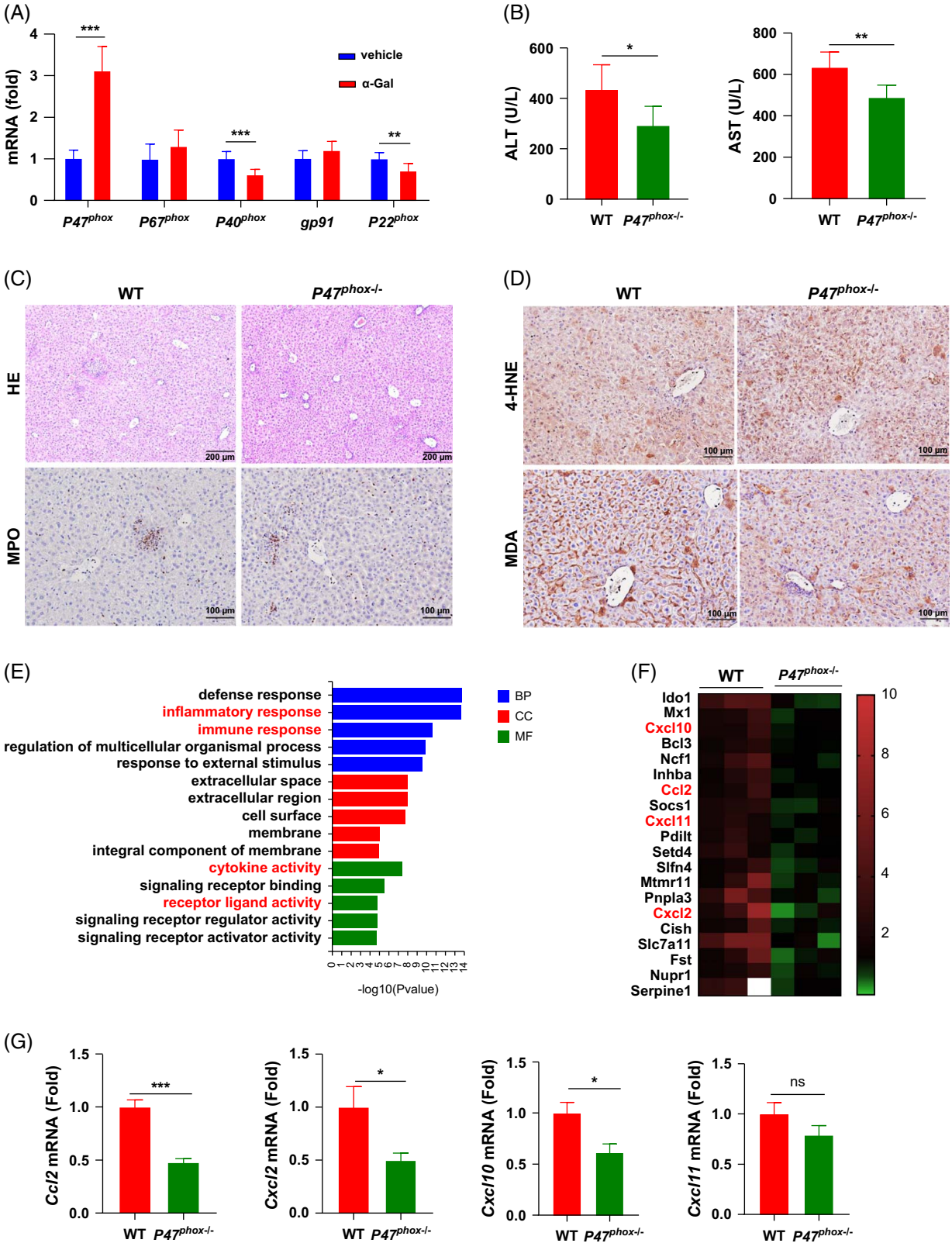

FIGURE 6 Neutrophils produce greater ROS by upregulating the expression of *P47phox*, thereby exacerbating α-Galcer–induced liver injury. (A) NADPH-associated molecule mRNA levels in isolated liver neutrophils were analyzed by RT-qPCR. (B) The expression levels of ALT and AST in serum were detected in WT and *P47phox−/−* mice by a biochemical reagent kit. (C) The infiltrating inflammatory cells in liver tissue were observed by H&E staining. And MPO+ neutrophils were detected by IHC staining. (D) Immunohistochemical staining to detect the expression levels of MDA and 4-HNE in liver tissue. (E) GO enrichment analysis of differentially expressed genes in mouse liver tissue. (F) Compared with WT mice, the 20 genes with the most significant decrease in expression in Ncf1−/− mice were ranked by *p* value. (G) The expression of *Ccl2*, *Cxcl2*, *Cxcl10*, and

Cxcl11 in the liver of WT mice and *P47^{phox}* mice after α-Galcer treatment. *$p < 0.05$, **$p < 0.01$, ***$p < 0.001$. Abbreviations: 4-HNE, 4-hydroxynonenal; H&E, hematoxylin-eosin; IHC, immunohistochemical; MDA, malondialdehyde; ROS, reactive oxygen species; RT-qPCR, reverse transcription-quantitative polymerase chain reaction; WT, wild-type.

stimulation of IL-2 and α-Galcer in vitro.[22] Th2 cytokines IL-4 and IL-13 participate in the regression of inflammation, which can promote M2 activation of macrophages in the liver, thus reducing liver injury.[23] TNF-α and IL-6 are 2 types of inflammatory cytokines, which can promote the development of inflammation. The increase of other cytokines (such as IL-5, IL-17A, IL-22) may be caused by changes in immune microenvironment. The disorder of these cytokines and chemokines mainly contributes to liver injury caused by α-Galcer.

In addition, many chemokines also have an obvious change in serum after α-Galcer treatment. CXCL1 is one of the most important chemokines, which is involved in the development of many inflammatory diseases. Accumulating studies have shown that CXCL1 was expressed in hepatocytes[24] and also in myeloid cells such as macrophages and mast cells.[25] CXCL1 can highly activate chemokine (C-X-C Motif) receptor 2 (CXCR2) and mediates the migration of neutrophils to inflammatory and necrotic regions. The high expression of CXCL1 in serum and the accumulation of neutrophils in the liver were found in our study. Interestingly, neutrophil accumulation is reduced by the CXCR2 inhibitor, which inhibits α-Galcer–induced liver injury, suggesting that CXCL1-CXCR2 axis–mediated hepatic neutrophil migration leads to liver injury. MCP-1, also known as chemokine (CC-motif) ligand 2 (CCL2), and its main function is to recruit monocytes/macrophages to the site of inflammation.[26] CCL2 is mainly secreted by monocytes and dendritic cells,[27] and is also expressed in hepatocytes.[28] CCR2, chemokine (C-C motif) receptor 2, is the receptor of MCP-1. Macrophages often infiltrate the liver through the CCL2-CCR2 axis and cause inflammatory damage.[29] Besides MCP-1, MIP-1β, MIP-1α, and RANTES also can mediate the migration of macrophages. An interesting study showed that MIP-1β could recruit bone marrow–derived monocytes to promote intraretinal revascularization and thus prevent abnormal NV in ischemic vision–threatening retinal diseases.[30] MIP-1α and MIP-1β are closely related to macrophage accumulation in the kidney and can aggravate mesangio proliferative glomerulonephritis.[31] RANTES, also called chemokine C-C ligand 5 (CCL5), is primarily secreted by T cells.[32] CCL5 can recruit CCR5$^+$ macrophages to the site of residual tumor cells and induce tumor recurrence.[33] In this current study, we demonstrated that inhibition of CCR5 signaling significantly alleviates α-Galcer–induced liver injury and inflammation. Interestingly, it has been reported that loss of CCL5 enhances CXCL1 expression in hepatocytes and activate CXCL1-CXCR2 axis in neutrophils to augment their hepatic migration, thus worsening NKT cell–mediated liver injury.[11] This different conclusion about the role of CCL5/CCR5 signaling in NKT cell hepatitis due to CCR5 is also shared by MIP-1β, MIP-1α, and RANTES. Another evidence is that CCR2 inhibitor or CCR5 inhibitor can not only reduce macrophage accumulation in the liver after α-Galcer injection but also limit neutrophil infiltration. Neutrophils are able to migrate to the liver through CCR2 and CCR5 in diclofenac-induced mouse liver injury.[34] Grommes et al[35] revealed that CCR2 could mediate neutrophil recruitment to inflamed lungs.[35] Taken together, these chemokines-driven macrophage/neutrophil infiltration is required for NKT cell–mediated hepatitis.

ROS was also referred to as the “respiratory burst” or “oxidative burst,” which was regarded as the most important ability for neutrophils to resistance to bacterial infection and virus invasion[36]; however, the excessive production of ROS from neutrophils, which is released in the external surroundings, can lead to tissue damage. Our results demonstrated that neutrophils activate NOX2 through the upregulation of p47phox mRNA to release excessive ROS, leading to liver injury. miR-223 is well known to play a key role in limiting neutrophil activation and chemotaxis.[37] Li et al[8] found that chronic-plus-binge ethanol feeding can exacerbate liver injury in mice by enhancing the IL-6–p47phox–oxidative stress pathway in neutrophils, but this process can be inhibited by miR-223. Ren et al showed that neutrophil-specific miR-223 downregulates the production of ROS in alcohol-associated liver disease and is influenced by upstream SIRT1 during aging.[38] For NKT cell–mediated hepatitis, the absence of miR-223 aggravates the production of ROS and liver injury. Those studies strongly declare the critical role of miR-223 to ameliorate ROS-induced liver injury.

MiR-223 is considered a myeloid cell-specific miRNA[39] and is highly expressed in neutrophils and monocytes.[40,41] Accumulating studies have shown that miR-223 can limit the excessive activation of neutrophils, and miR-223–deficient neutrophils are more susceptible to inflammatory responses.[8,42] For example, miR-223 derived from the myeloid cells regulated intestinal inflammation by inhibiting NLRP3 inflammasome.[43] In addition, NCF1 expressed by myeloid cells is involved in the progression of different diseases.[44,45] NCF1 plays a key role in controlling ROS production in neutrophils, and its upregulation is closely related to liver inflammation.[46] Macrophages could inhibit T-cell responses and the development of arthritis through NCF1-mediated ROS production.[47] These studies strongly emphasize the

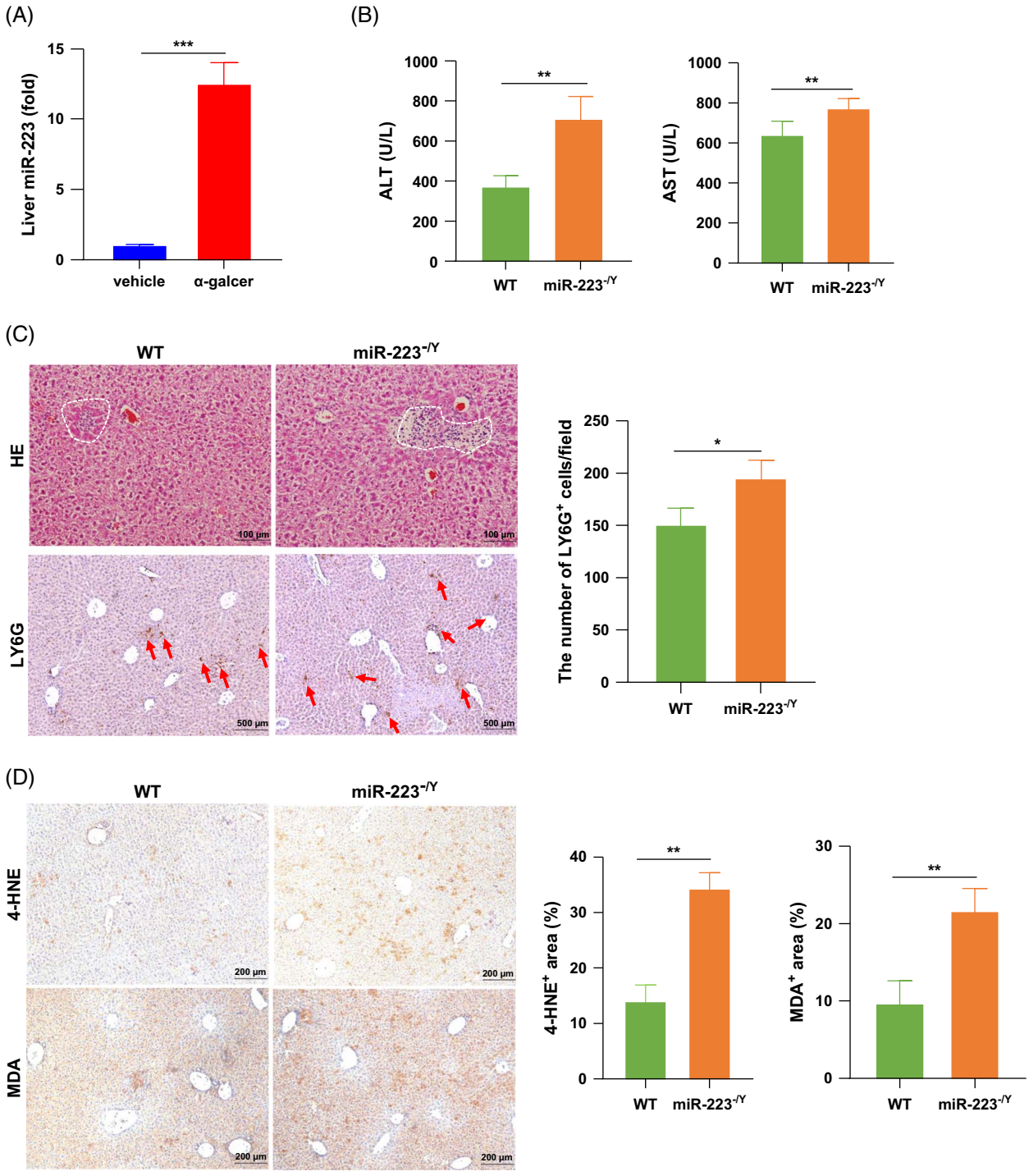

FIGURE 7 The absence of miR-223 causes a worse liver injury after α-Galcer injection. WT and miR-223 knockout (miR-223$^{-/Y}$) mice were treated with α-Galcer for 16 hours. Serum and liver tissue samples were collected. (A) The hepatic levels of miR-223 were analyzed by RT-qPCR. (B) The levels of ALT and AST in serum were measured. (C) Neutrophil and other inflammatory cell infiltration in the liver were analyzed by H&E staining and Ly6G staining. The quantitation of Ly6G$^+$ cells per field was determined. (D) The levels of MDA and 4-HNE were determined by immunohistochemical staining. Representative images are shown. The quantitation of MDA$^+$ and 4-HNE$^+$ area per field was determined. Values represent means ± SD. *$p < 0.05$, **$p < 0.01$, ***$p < 0.001$. Abbreviations: 4-HNE, 4-hydroxynonenal; H&E, hematoxylin-eosin; MDA, malondialdehyde; RT-qPCR, reverse transcription-quantitative polymerase chain reaction; WT, wild-type.

important roles of miR-223 and NCF1 in myeloid cells. It is reasonable that the phenotypes observed in miR-223 and NCF1-deficient mice after α-Galcer injection may be due to the effect of miR-223 and NCF1 on myeloid cells.

The release of proinflammation cytokines from macrophages and the recruitment of inflammation cells by macrophages are regarded as the main reasons leading to liver injury. KCs recruit neutrophils and

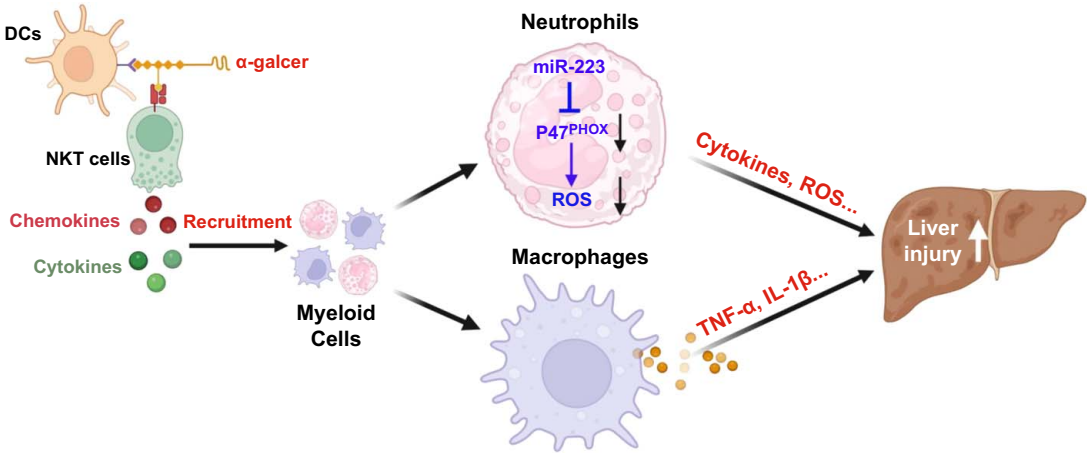

FIGURE 8 A model depicting the critical roles of myeloid cells and KCs in α-Galcer–induced NKT cell hepatitis. NKT cell activation after α-Galcer injection results in the elevation of several hepatic myeloid cell infiltration–related cytokines and chemokines. Neutrophil and monocyte-derived macrophage infiltration promotes α-Galcer–induced liver injury by the release of ROS and proinflammatory mediators. Inhibition of neutrophil or macrophage migration ameliorates liver injury and inflammation. Interestingly, neutrophils promote ROS production and exacerbate liver damage by upregulating the expression of *Ncf1*. Meanwhile, anti-inflammatory and oxidative stress miR-223 protects against α-Galcer–mediated liver injury by limiting ROS production and inflammation. Abbreviations: α-Galcer, α-Galactosylceramide; NKT, natural killer T; ROS, reactive oxygen species.

inflammatory monocytes to infiltrate the liver by secreting IL-1 α, exacerbating APAP-induced liver injury.[48] Monocyte-derived macrophages are a major type of inflammatory cells, and inhibiting the infiltration of monocytes can significantly improve steatohepatitis and liver fibrosis.[49] A new study suggests that $CXCL2^+$ macrophages can secrete TNF-α and IL-1β to stimulate the formation of neutrophil extracellular traps, thereby exacerbating liver damage.[50] Our results indicate that using CCR2 and CCR5 inhibitors to block the CCL2-CCR2 axis and CCL5-CCR5 axis can significantly reduce the infiltration of monocytes in the liver and improve α-Galcer–induced liver injury.

In summary, our data reveal that neutrophils and macrophages are accumulated in α-Galcer–induced liver injury. Neutrophils release excessive ROS by upregulating the expression of *Ncf1* to induce liver injury, and the absence of miR-223 would exacerbate the damage caused by ROS. These findings reveal a novel mechanism for NKT cell–mediated hepatitis and have implications for the application of NKT cell therapy.

FUNDING INFORMATION

This work was partly supported by the National Natural Science Foundation of China (Nos. 82074155, 82274467, 82270601, China); Program of Shanghai Academic/Technology Research Leader (No. 20XD1423500, China); Shanghai Frontier Research Base of Disease and Syndrome Biology of inflammatory cancer transformation (No. 2021KJ03-12, China); Shanghai Collaborative Innovation Center of Industrial Transformation of Hospital TCM Preparation (China); and Natural Science Foundation of Shanghai (22ZR1473800).

CONFLICTS OF INTEREST

The authors have no conflicts to report.

REFERENCES

1. Kubes P, Jenne C. Immune responses in the liver. Annu Rev Immunol. 2018;36:247–77.
2. T K. CD1d-restricted and TCR-mediated activation of Va14 NKT cells by glycosylceramides. Science. 1997;278:1626–9.
3. MJ S. NKT cells and tumor immunity—A double-edged sword. Nat Immunol. 2000;1:459–60.
4. Wang H, Yin S. Natural killer T cells in liver injury, inflammation and cancer. Expert Rev Gastroenterol Hepatol. 2015;9:1077–85.
5. Paul S, Chhatar S, Mishra A, Lal G. Natural killer T cell activation increases iNOS(+)CD206(-) M1 macrophage and controls the growth of solid tumor. J Immunother Cancer. 2019;7:208.
6. Kolaczkowska E, Kubes P. Neutrophil recruitment and function in health and inflammation. Nat Rev Immunol. 2013;13:159–75.
7. Hwang S, He Y, Xiang X, Seo W, Kim SJ, Ma J, et al. Interleukin-22 ameliorates neutrophil-driven nonalcoholic steatohepatitis through multiple targets. Hepatology. 2020;72:412–29.
8. Li M, He Y, Zhou Z, Ramirez T, Gao Y, Gao Y, et al. MicroRNA-223 ameliorates alcoholic liver injury by inhibiting the IL-6-p47 (phox)-oxidative stress pathway in neutrophils. Gut. 2017;66:705–15.
9. He Y, Rodrigues RM, Wang X, Seo W, Ma J, Hwang S, et al. Neutrophil-to-hepatocyte communication via LDLR-dependent miR-223-enriched extracellular vesicle transfer ameliorates nonalcoholic steatohepatitis. J Clin Invest. 2021;131:e141513.
10. Yang W, Tao Y, Wu Y, Zhao X, Ye W, Zhao D, et al. Neutrophils promote the development of reparative macrophages mediated by ROS to orchestrate liver repair. Nat Commun. 2019;10:1076.
11. Chen L, Gu J, Qian Y, Li M, Qian Y, Xu M, et al. Deletion of C-C motif chemokine ligand 5 worsens invariant natural killer T-cell-mediated hepatitis via compensatory up-regulation of CXCR2-related chemokine activity. Cell Mol Gastroenterol Hepatol. 2019;7:623–39.
12. Wang H, Feng D, Park O, Yin S, Gao B. Invariant NKT cell activation induces neutrophil accumulation and hepatitis:

Opposite regulation by IL-4 and IFN-gamma. Hepatology. 2013; 58:1474–85.
13. Peng J, Li J, Huang J, Xu P, Huang H, Liu Y, et al. p300/CBP inhibitor A-485 alleviates acute liver injury by regulating macrophage activation and polarization. Theranostics. 2019;9: 8344–61.
14. Li M, Sun X, Zhao J, Xia L, Li J, Xu M, et al. CCL5 deficiency promotes liver repair by improving inflammation resolution and liver regeneration through M2 macrophage polarization. Cell Mol Immunol. 2020;17:753–64.
15. Tacke F, Zimmermann HW. Macrophage heterogeneity in liver injury and fibrosis. J Hepatol. 2014;60:1090–6.
16. Zhang XW, An MX, Huang ZK, Ma L, Zhao D, Yang Z, et al. Lpp of Escherichia coli K1 inhibits host ROS production to counteract neutrophil-mediated elimination. Redox Biol. 2023;59:102588.
17. Dorhoi A, Iannaccone M, Farinacci M, Fae KC, Schreiber J, Moura-Alves P, et al. MicroRNA-223 controls susceptibility to tuberculosis by regulating lung neutrophil recruitment. J Clin Invest. 2013;123:4836–48.
18. Bedard M, Salio M, Cerundolo V. Harnessing the power of invariant natural killer T cells in cancer immunotherapy. Front Immunol. 2017;8:1829.
19. King LA, Lameris R, de Gruijl TD, van der Vliet HJ. CD1d-invariant natural killer T cell-based cancer immunotherapy: Alpha-Galactosylceramide and beyond. Front Immunol. 2018;9: 1519.
20. Bandyopadhyay K, Marrero I, Kumar V. NKT cell subsets as key participants in liver physiology and pathology. Cell Mol Immunol. 2016;13:337–46.
21. Wang F, Zhang S, Jeon R, Vuckovic I, Jiang X, Lerman A, et al. Interferon gamma induces reversible metabolic reprogramming of M1 macrophages to sustain cell viability and pro-inflammatory activity. EBioMedicine. 2018;30:303–16.
22. Iizuka A, Ikarashi Y, Yoshida M, Heike Y, Takeda K, Quinn G, et al. Interleukin (IL)-4 promotes T helper type 2-biased natural killer T (NKT) cell expansion, which is regulated by NKT cell-derived interferon-gamma and IL-4. Immunology. 2008;123: 100–7.
23. Feng XX, Chi G, Wang H, Gao Y, Chen Q, Ru YX, et al. IL-37 suppresses the sustained hepatic IFN-gamma/TNF-alpha production and T cell-dependent liver injury. Int Immunopharmacol. 2019;69:184–93.
24. Deng Y, Zhao Z, Sheldon M, Zhao Y, Teng H, Martinez C, et al. LIFR regulates cholesterol-driven bidirectional hepatocyte-neutrophil cross-talk to promote liver regeneration. Nat Metab. 2024; 6:1756–74.
25. De Filippo K, Dudeck A, Hasenberg M, Nye E, van Rooijen N, Hartmann K, et al. Mast cell and macrophage chemokines CXCL1/CXCL2 control the early stage of neutrophil recruitment during tissue inflammation. Blood. 2013;121:4930–7.
26. Singh S, Anshita D, Ravichandiran V. MCP-1: Function, regulation, and involvement in disease. Int Immunopharmacol. 2021;101(pt B):107598.
27. Serbina NV, Jia T, Hohl TM, Pamer EG. Monocyte-mediated defense against microbial pathogens. Annu Rev Immunol. 2008; 26:421–52.
28. Li X, Yuan B, Lu M, Wang Y, Ding N, Liu C, et al. The methyltransferase METTL3 negatively regulates nonalcoholic steatohepatitis (NASH) progression. Nat Commun. 2021;12: 7213.
29. Baeck C, Wehr A, Karlmark KR, Heymann F, Vucur M, Gassler N, et al. Pharmacological inhibition of the chemokine CCL2 (MCP-1) diminishes liver macrophage infiltration and steatohepatitis in chronic hepatic injury. Gut. 2012;61:416–26.
30. Ishikawa K, Yoshida S, Nakao S, Sassa Y, Asato R, Kohno R, et al. Bone marrow-derived monocyte lineage cells recruited by MIP-1beta promote physiological revascularization in mouse model of oxygen-induced retinopathy. Lab Invest. 2012;92: 91–101.
31. Wang W, Qian B, Zhao C, Peng M, Liu L, Xie M, et al. Sublytic C5b-9 induces CCL3/4 production and macrophage accumulation in Thy-1N rats via PKC-alpha/p65/IRF-8 axis. Int J Biol Sci. 2022;18:3178–93.
32. Hu A, Zhu J, Zeng C, Lin CH, Yu J, Liu JQ, et al. IL-27 Induces CCL5 production by T lymphocytes, which contributes to antitumor activity. J Immunol. 2022;208:2239–45.
33. Walens A, DiMarco AV, Lupo R, Kroger BR, Damrauer JS, Alvarez JV. CCL5 promotes breast cancer recurrence through macrophage recruitment in residual tumors. Elife. 2019;8: e43653.
34. He Z, Wei G, Li N, Niu M, Gong S, Wu G, et al. CCR2 and CCR5 promote diclofenac-induced hepatotoxicity in mice. Naunyn Schmiedebergs Arch Pharmacol. 2019;392:287–97.
35. Grommes J, Drechsler M, Soehnlein O. CCR5 and FPR1 mediate neutrophil recruitment in endotoxin-induced lung injury. J Innate Immun. 2014;6:111–6.
36. El-Benna J. Priming of the neutrophil respiratory burst: Role in host defense and inflammation. Immunol Rev. 2016;273: 180–293.
37. Wang X, He Y, Mackowiak B, Gao B. MicroRNAs as regulators, biomarkers and therapeutic targets in liver diseases. Gut. 2021; 70:784–95.
38. Ren R, He Y, Ding D, Cui A, Bao H, Ma J, et al. Aging exaggerates acute-on-chronic alcohol-induced liver injury in mice and humans by inhibiting neutrophilic sirtuin 1-C/EBPalpha-miRNA-223 axis. Hepatology. 2022;75:646–60.
39. Cantoni C, Cignarella F, Ghezzi L, Mikesell B, Bollman B, Berrien-Elliott MM, et al. Mir-223 regulates the number and function of myeloid-derived suppressor cells in multiple sclerosis and experimental autoimmune encephalomyelitis. Acta Neuropathol. 2017;133:61–77.
40. Bauernfeind F, Rieger A, Schildberg FA, Knolle PA, Schmid-Burgk JL, Hornung V. NLRP3 inflammasome activity is negatively controlled by miR-223. J Immunol. 2012;189: 4175–81.
41. Johnnidis JB, Harris MH, Wheeler RT, Stehling-Sun S, Lam MH, Kirak O, et al. Regulation of progenitor cell proliferation and granulocyte function by microRNA-223. Nature. 2008;451: 1125–9.
42. He Y, Feng D, Li M, Gao Y, Ramirez T, Cao H, et al. Hepatic mitochondrial DNA/Toll-like receptor 9/MicroRNA-223 forms a negative feedback loop to limit neutrophil overactivation and acetaminophen hepatotoxicity in mice. Hepatology. 2017;66: 220–34.
43. Neudecker V, Haneklaus M, Jensen O, Khailova L, Masterson JC, Tye H, et al. Myeloid-derived miR-223 regulates intestinal inflammation via repression of the NLRP3 inflammasome. J Exp Med. 2017;214:1737–52.
44. Zhong J, Li Q, Luo H, Holmdahl R. Neutrophil-derived reactive oxygen species promote tumor colonization. Commun Biol. 2021;4:865.
45. Pinel-Marie ML, Sparfel L, Desmots S, Fardel O. Aryl hydrocarbon receptor-dependent induction of the NADPH oxidase subunit NCF1/p47 phox expression leading to priming of human macrophage oxidative burst. Free Radic Biol Med. 2009;47: 825–34.
46. Ma J, Guillot A, Yang Z, Mackowiak B, Hwang S, Park O, et al. Distinct histopathological phenotypes of severe alcoholic hepatitis suggest different mechanisms driving liver injury and failure. J Clin Invest. 2022;132:e157780.
47. Gelderman KA, Hultqvist M, Pizzolla A, Zhao M, Nandakumar KS, Mattsson R, et al. Macrophages suppress T cell responses and arthritis development in mice by producing reactive oxygen species. J Clin Invest. 2007;117:3020–8.

48. Zhang C, Feng J, Du J, Zhuo Z, Yang S, Zhang W, et al. Macrophage-derived IL-1alpha promotes sterile inflammation in a mouse model of acetaminophen hepatotoxicity. Cell Mol Immunol. 2018;15:973–82.
49. Krenkel O, Puengel T, Govaere O, Abdallah AT, Mossanen JC, Kohlhepp M, et al. Therapeutic inhibition of inflammatory monocyte recruitment reduces steatohepatitis and liver fibrosis. Hepatology. 2018;67:1270–83.
50. Liu Y, Xiao J, Cai J, Li R, Sui X, Zhang J, et al. Single-cell immune profiling of mouse liver aging reveals Cxcl2+ macrophages recruit neutrophils to aggravate liver injury. Hepatology. 2024;79:589–605.

How to cite this article: Tan J, Ji L, Li Q, Guo R, Hao Y, Xiao P, et al. Multiple Cell-type interactions drive invariant NKT cell hepatitis. Hepatol Commun. 2025;9:e0592. https://doi.org/10.1097/HC9.0000000000000592